Environ Monit Assess (2022) 194: 456
https://doi.org/10.1007/s10661-022-10107-7

Health risk assessment of gaseous elemental mercury (GEM) in Mexico City

Benedetto Schiavo · Ofelia Morton-Bermea · Elias Salgado-Martínez · Rocío García-Martínez · Elizabeth Hernández-Álvarez

Received: 3 December 2021 / Accepted: 15 May 2022 / Published online: 25 May 2022

Abstract Emissions of gaseous elemental mercury (GEM or Hg^0) from different sources in urban areas are important subjects for environmental investigations. In this study, atmospheric Hg measurements were conducted to investigate air pollution in the urban environment by carrying out several mobile surveys in Mexico City. This work presents atmospheric concentrations of GEM in terms of diurnal variation trends and comparisons with criteria for pollutant concentrations such as CO, SO_2, NO_2, $PM_{2.5}$, and PM_{10}. The concentration of GEM was measured during the pre-rainy period by using a high-resolution active air sampler, the Lumex RA 915 M mercury analyzer. In comparison with those for other cities worldwide, the GEM concentrations were similar or slightly elevated, and they ranged from 0.20 to 30.23 ng m^{-3}. However, the GEM concentration was significantly lower than those in contaminated areas, such as fluorescent lamp factory locations and gold mining zones. The GEM concentrations recorded in Mexico City did not exceed the WHO atmospheric limit of 200 ng m^{-3}. We performed statistical correlation analysis which suggests equivalent sources between Hg and other atmospheric pollutants, mainly NO_2 and SO_2, emitted from urban combustion and industrial plants. The atmospheric Hg emissions are basically controlled by sunlight radiation, as well as having a direct relationship with meteorological parameters. The area of the city studied herein is characterized by high traffic density, cement production, and municipal solid waste (MSW) treatment, which constantly release GEM into the atmosphere. In this study, we included the simulation with the HYSPLIT dispersion model from three potential areas of GEM release. Emissions from industrial corridors and volcanic plumes localized outside the urban area contribute to the pollution of Mexico City and mainly affect the northern area during specific periods and climate conditions. Using the USEPA model, we assessed the human health risk resulting from exposure to inhaled GEM among residents of Mexico City. The results of the health risk assessment indicated no significant noncarcinogenic risk (hazard quotient (HQ) < 1) or consequent adverse effects for children and adults living in the sampling area over the study period. GEM emissions inventory data is necessary to improve our knowledge about the Hg contribution and effect in urban megacity areas with the objective to develop

Supplementary information The online version contains supplementary material available at https://doi.org/10.1007/s10661-022-10107-7.

B. Schiavo (✉) · O. Morton-Bermea · E. Salgado-Martínez · E. Hernández-Álvarez
Instituto de Geofísica, Universidad Nacional Autónoma de México, 04150 Mexico City, DF, Mexico
e-mail: benedetto@igeofisica.unam.mx

R. García-Martínez
Instituto de Ciencias de la Atmósfera y Cambio Climático, Universidad Nacional Autónoma de México, 04150 Mexico City, DF, Mexico

public safe policy and implementing the Minamata Convention.

Keywords Gaseous elemental mercury · Mexico City · Mercury pollution · Dispersion model · Health risk · Lumex

Introduction

Mercury (Hg) is an important trace element and is of global concern due to its high toxicity and significant adverse effects that can impact the ecosystem and human health (U.S. Department of Health and Human Services, Public Health Service, ATSDR, 2012; Budnik & Casteleyn, 2019; Hylander & Goodsite, 2005). Hg is involved in a complex biogeochemical cycle that includes emissions from natural and anthropogenic sources, oxidation/reduction in gaseous and aqueous phases, and finally deposition and re-emission in the atmosphere (Gustin et al., 2020). Hg can remain in the atmosphere for a long time (0.5 to 2 years) and can be transported over long distances away from sources (Gworek et al., 2017; Lyman et al., 2020; Schroeder & Munthe, 1998). Input of atmospheric Hg from natural sources includes volcanic emissions (Schiavo et al., 2020a; Edwards et al., 2021), and anthropogenic release mainly comes from coal-fired power plants, fossil fuel combustion, and artisanal gold mining (Pirrone et al., 2010; Sprovieri et al., 2010). Thus, potential exposure to Hg may affect the world's population and ecosystems, even in remote areas, e.g., Arctic and Antarctic regions (Angot et al., 2016; Bargagli, 2016). The Minamata Convention, approved by the United Nations and agreed upon by more than 120 governments around the world, is designed to monitor Hg in the atmosphere, soil, and water, reduce anthropogenic emissions of Hg compounds, and protect the environment (Bank, 2020; UNEP, 2013).

Inorganic Hg appears in three oxidation states in nature: Hg^0 (elemental mercury), Hg^+ (mercurous), and Hg^{2+} (mercuric). Hg^0, also known as gaseous elemental mercury (GEM), is the typical and most abundant form of Hg present in the atmosphere. This form is characterized by low solubility and high vapor pressure, which make it toxic and harmful to health. GEM is mainly absorbed in the lungs (~ 80%) (Park & Zheng, 2012) and can spread throughout the body, cross the blood–brain barrier, and accumulate in the central nervous system (Bjørklund et al., 2017). Hg^+ is not stable under normal environmental conditions and is rarely observable. Hg^{2+}, usually known as reactive gaseous mercury (RGM), is the common oxidized form of Hg that is rapidly absorbed on the surfaces of raindrop particles and deposited on the Earth's surface by wet and dry deposition processes (Li et al., 2020). The lifetime of RGM in the atmosphere is significantly shorter than that of GEM, approximately hours to days (Swartzendruber et al., 2006). Park and Zheng (2012) reported that the level of RGM absorption in the human body caused by inhalation was approximately 50% lower than that of GEM. However, absorption by ingestion was higher than that of GEM (0.01%), in the range 7–14%.

Exposure to toxic levels of Hg compounds is related to neurological disorders, respiratory syndrome, cardiovascular complications, and genetic damage (Berlin et al., 2015). Methylmercury (MeHg) is the most hazardous organic form of Hg and is considered a potent neurotoxicant (dos Santos et al., 2016). Aquatic microorganisms catalyze biomethylation of inorganic Hg to produce MeHg (Hintelmann, 2010). MeHg can be found in various sources, such as fish, pesticides, and fungicides. The gastrointestinal tract absorbs approximately 95% of the MeHg ingested, mainly during the consumption of seafood (Heidari-Beni et al., 2015; dos Santos et al., 2016). Several health effects were reported in a population located near an artisanal gold mining area (Esdaile & Chalker, 2018). Bose-O'Reilly et al. (2008) recognized several diseases, such as kidney, neurological, and autoimmune effects, in children who worked in gold ore extraction and lived in the area. Gold mining communities are exposed to high levels of Hg vapor and MeHg, as evidenced by blood, urine, and hair concentrations of Hg (Gibb & O'Leary, 2014).

In Mexico, observations of atmospheric Hg levels in urban, industrial, and mining areas have been reported in some studies (e.g., de la Rosa et al., 2004; Fuentes García et al., 2017; Velasco et al., 2016; Morton-Bermea et al., 2021a). GEM concentrations registered in Mexican mining zones ranged from 40 (García-Martínez et al., 2021) to 71.8 ng m^{-3} (de la Rosa et al., 2004), higher than levels observed close to coal-fired power plants (Fuentes García et al., 2017) and non-contaminated areas (Velasco et al., 2016), approximately 2.8 and 1.04 ng m^{-3}, respectively. The first studies on atmospheric Hg levels in Mexico City were conducted in the early twenty-first century. In Mexico City, de la Rosa et al. (2004) reported

GEM concentrations of 9.8 ng m^{-3} during several survey measurements. On the other hand, atmospheric Hg measurements made close to municipal solid waste (MSW) dumps in Mexico City (de la Rosa et al., 2006) were characterized by elevated concentrations of GEM ranging from 12.5 to 1282.3 ng m^{-3}. Rutter et al. (2009) investigated GEM levels at fixed stations during real-time measurements recorded in the Mexico City Metropolitan Area (MCMA) and reported values of 7.2 ng m^{-3}. Recently, Morton-Bermea et al. (2021b) examined GEM concentrations with two road surveys in MCMA realized in different sampling periods, and they recorded average values of 4.42 ng m^{-3}.

To date, considering the population density, pollution, and industrial development, few studies of Hg vapor concentration and spatial distribution have been conducted in Mexico City. Many studies focus in atmospheric Hg transport reports primarily local sources; however, regional transport from multiple sources plays an important role in the dispersion of GEM in the urban environment. The transport models allow improving the investigation on the dispersion of contaminants and are essential for targeted control of GEM. According to our knowledge, the potential health risk of atmospheric Hg in the Mexico City is reported for the first time. The objectives of this study were (i) to measure ambient GEM concentrations and speciation with passive air sampling at five different surveys in Mexico City during the pre-rainy season, (ii) to investigate the spatiotemporal distribution of GEM, (iii) to identify potential sources of atmospheric Hg, and (iv) to determine the health risks of human Hg exposure.

Materials and methods

Study area and methodology

Mexico City is located in the Valley of Mexico (19° 26′N 99°8′W) and is the capital and largest megacity of Mexico (1485 km^2) (Fig. 1). According to the statistical census of 2020 (INEGI, 2020), the population was approximately 9 million; this value increases when the metropolitan area is considered, since it houses more than 21 million inhabitants. The studied area is characterized by highly traffic density and urbanization, with uncontrolled development over the past 30 years. The industrial district is situated in the northern part of the city with high population density. Meanwhile, the center and southern part of the study area has been dominated by commercial and residential activity with high traffic index (Morton-Bermea et al., 2015). In Mexico City, the climate is subtropical (warm and temperate), classified as Cwb with the Köppen climate classification (Estrada et al., 2009; Ostad-Ali-Askar et al., 2018). The average annual temperature varies from 12 to 16 °C, with a daily average temperature of ~ 17 °C. The warmest month of the year is May, with an average temperature of ~ 19 °C. The seasons are well defined and generally separated into three periods: (i) the cool dry season, also known as the post-rainy period (from mid-October to February), (ii) the warm, dry season, also known as the pre-rainy period (from March to May), and (iii) the rainy season, which is concentrated mainly in the summer and is characterized by rainfall that exceeds 100 mm per month (from June to mid-October).

The monitoring campaign ran from March to June 2021 (warm-dry period), and 5 surveys were carried out around Mexico City during working days in which schools were closed and offices were operating in dual presential and smart working modes; this was done in an effort to contain the recent COVID-19 global pandemic. During the pre-rainy season, we investigated diurnal variations in GEM released into the atmosphere. The observations were conducted mainly over central hours of the day, when solar radiation and air temperature increase (Gustin, 2003; Sizmur et al., 2017; Talebmorad et al., 2021). The monitoring areas were chosen to include residential areas, commercial establishments, waste dumps, and industrial complexes. GEM concentrations are influenced by emissions from heavy traffic, asphalt plants, and the cement industry. Under certain environmental conditions, emissions from industrial complexes, e.g., Tula-Tepeji (Retama et al., 2019) and Apaxco, and the plume of the Popocatépetl volcano (Schiavo et al., 2020a), located 60 km north-northwest and 70 km southeast of Mexico City, respectively, affected the atmospheric urban environment and contributed to air pollution.

Instrumentation

During our survey, we measured GEM concentrations in the atmospheric environment of five road transects distributed within different areas of Mexico City (Fig. 1). The surveys were carried out in different periods of

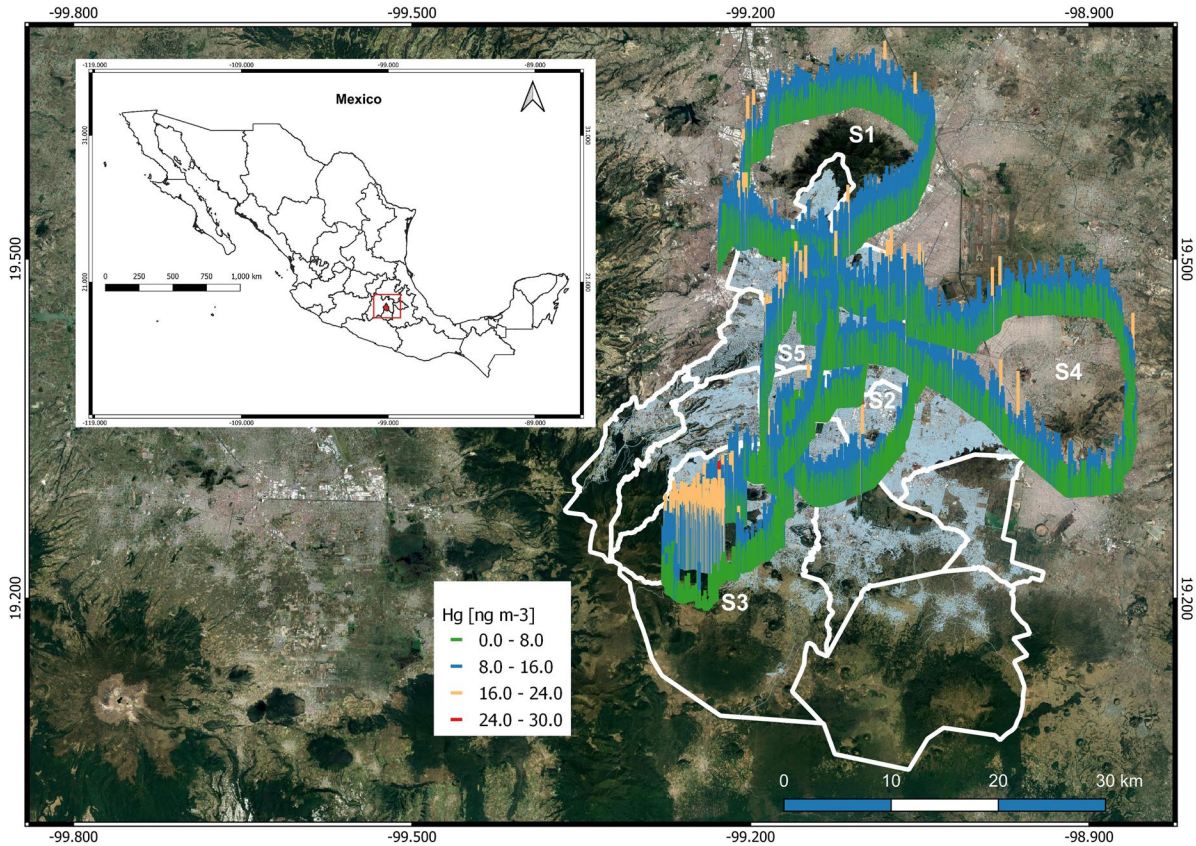

Fig. 1 GEM concentrations measured during 5 road cars' transect around the Mexico City study area. Sample survey keys (S1 to S5) are also reported

2021 through the warm, dry season: (i) March 31, (ii) April 17, (iii) May 8 and 9, and (iv) June 27. GEM concentrations in the urban environment were determined by using a Lumex RA 915 M, a portable vapor analyzer for continuous Hg measurements, which was calibrated by the manufacturer (in this article, GEM and Hg are used without distinction). Although Tekran (Lindberg et al., 2007; Sprovieri et al., 2010) and amalgamation methods with gold traps (Gustin et al., 2015) satisfy high international standards (QA/QC) and are applied for fixed observation network stations worldwide, their use is limited by poor portability and the employment of reference materials during analytical procedures, among other factors. The overarching objective of the Global Mercury Observation System to establish a global Hg monitoring network was achieved while keeping in mind the need to assure high-quality observations in line with international quality assurance/quality control (QA/QC) standards and to fill the gap in terms of spatial coverage of measurements in the Southern Hemisphere where data were lacking or nonexistent. Lumex provides important instrumental and logistical improvements in comparison to other analytical techniques used for Hg monitoring. The analytical procedure is based on differential Zeeman atomic absorption spectrometry (ZAAS) at 254 nm and is characterized by polarized light, high-frequency modulation, and interference-free measurements. Measurement sensitivity and selectivity were provided by Zeeman background correction and a multipath analytical cell (Sholupov & Ganeyev, 1995). The instrument collects air samples at a controlled flow rate of 10 L m^{-1}, and Hg concentrations are directly available in real time and visualized on a digital display. The analytical technique presents various advantages; it is portable, operates with different climatic conditions such as low temperature and high relative humidity, has low

power consumption, performs automatic preconcentration, and does not require a special carrier gas or Teflon filter. The frequency for data acquisition was adjusted to 1 s, and a zero correction was applied every 20 min to reset the baseline. Lumex operates in a dynamic range, 0.5 to 20,000 ng m^{-3}, that covers several orders of magnitude. The detection limit was ~ 0.5 ng m^{-3}, and the instrumental accuracy of measurements was better than 95%. To compare our measurements with the background level of atmospheric GEM in the investigated area, we used the value reported by Morton-Bermea et al. (2021b), who estimated the GEM background in MCMA at approximately 2.53 ng m^{-3}. The whole procedure involved a Garmin GPS Map 60CSX for geographic location data acquisition.

Auxiliary data

Additionally, we provide information on standard meteorological parameters (including temperature (T), relative humidity (RH), wind speed (WS), and wind direction (WD)) and trace gases (particulate matter (PM), CO, NO_2, and SO_2), since many factors affecting the variability of GEM emissions include T, atmospheric turbulence, and sunlight, among others (Cizdziel et al., 2019; Zhou et al., 2020). Meteorological data and trace gas concentrations were downloaded from the Automated Atmospheric Monitoring Network (Red Automática de Monitoreo Atmosférico (RAMA) and Red de Meteorología y Radiación Solar (REDMET)) available at http://www.aire.cdmx.gob.mx/. RAMA air quality monitoring network used several instruments to determine the concentration of trace gases and PM. In particular, SO_2, NO_2, and CO are analyzed with Teledyne API system applying fluorescence, chemiluminescence, and gas filter correlation methods, respectively. On the other hand, Thermo Model 1405-DF instrument was employed to determine the PM concentration using gravimetric method that pumps air through two filters at constant flow rate, weighing the filters and calculating the mass concentration of PM in real time. The ground-based monitoring stations are distributed within the MCMA (Fig. S1) and provide hourly average concentrations of the main contaminants and climatological data. The collected datasets are consistent and in good agreement with the number of samples reported in other works and similar study areas, i.e., urban environments.

Transport contribution analysis

Forward plume dispersion simulations were carried out to identify potential sources of atmospheric Hg, and they considered three probable GEM pollution sources located outside the Mexico City area: (i) Tula-Tepeji industrial complex (20°02′55″N 99°16′19″W), (ii) Apaxco industrial corridor (19°59′00″N 99°10′00″W), and (iii) Popocatépetl volcano (19°01′20″N 98°37′40″W). The HYSPLIT trajectory model, developed in NOAA's Air Resources Laboratory, simulates atmospheric transport and dispersion using mesoscale meteorological data (Stein et al., 2015). Model calculations used a method that is a hybrid of the Lagrangian approach and Eulerian methodology, with a calculated error of approximately 15–30% (Draxler, 2008). However, model accuracy is dependent on the resolution of meteorological data. The simulation options and model evaluations used in this study included a Global Forecast System (GFS) with a 0.25-degree spatial horizontal resolution, a temporal resolution of 3 h, and an elevation of 500 m above ground level (AGL). The model was applied to the entire survey period. The grid inventory data of GEM emission sources and HYSPLIT dispersion trajectories were imported to QGIS (V. 3.16).

Health risk assessment

The health risk model, introduced by the United States—Environmental Protection Agency (USEPA), consists of several steps, including measurements and assessment, identification of exposure pathways, toxicity determination, and evaluation of human health risks (USDOE, 2011; USEPA, 1989). In this study, exposure of the population to Hg was considered for assessment and evaluation of noncarcinogenic risk (NCR). According to the International Agency for Research on Cancer (IARC), no human data relate elemental Hg exposure to cancer risk (Kim et al., 2015), but available data are limited. Local residents are exposed to GEM via inhalation through the nose and mouth of resuspended particles emitted from dust (USEPA, 2002).

The chronic exposure concentration (CEC) (ng m^{-3}) for atmospheric GEM ingested via inhalation was calculated as follows (USEPA, 2009; Gyamfi et al., 2020):

$$\mathrm{CEC_{Hg}} = \frac{C \times ET \times EF \times ED}{AT} \quad (1)$$

where C is the GEM concentration (ng·m^{-3}). Other specific factors and parameters used in the exposure risk assessment model were selected from the USEPA (2009) and are shown in Table S1. The noncarcinogenic health risk is expressed through the hazard quotient (HQ), which represents the probability of an individual suffering an adverse effect. HQ is calculated by normalization of the CEC_{Hg} and the affiliated reference toxicity dose for each metal(loid):

$$HQ = \frac{CEC_{Hg}}{RfC_{Hg}} \quad (2)$$

where RfC is the Hg reference dose for inhalation exposure (3×10^{-4} mg m^{-3}) (USEPA, 2020). As recommended by the USEPA (1989, 2001), if the HQ value is smaller than 1, there is no risk of noncarcinogenic adverse effects, and a HQ value exceeding 1 suggests the potential for noncarcinogenic risk to human health.

Statistical analysis

Correlations between GEM concentrations, meteorological parameters, and trace gas components were analyzed using the Spearman correlation coefficient. Statistical treatments of data, including graphical representations, were performed using Python version 3.7 and XLSTAT software. We used Quantum GIS to map GEM concentrations and applied a polynomial method to interpolate data. Significative differences were identified by $p < 0.05$.

Results and discussion

Atmospheric GEM concentrations

Descriptive statistics for GEM concentrations in each survey were collected in Mexico City before the rainy season and are shown in Table 1. The Hg present in the atmosphere was affected by local climate conditions. During the summer period (rainy season) in Mexico City, intense rain and strong winds impact the urban environment and influence the levels of GEM and other pollutants (Retama et al., 2015) through wet deposition and dispersion (Ostad-Ali-Askari & Shayannejad, 2021). Higher GEM concentrations were observed under calm wind conditions (Esbrí et al., 2014). The GEM concentrations over the entire study period ranged from 0.20 to 30.23 ng m^{-3} (N=27,126), with an average value of 5.60±2.33 ng m^{-3} and a median of 5.08 ng m^{-3} (Fig. S2). The first survey (S1, N=6652), conducted in the northern area of the city characterized by an industrial complex and heavy road traffic, recorded an average GEM concentration of 5.62±2.03 ng m^{-3} (maximum of 18.30 ng m^{-3}). During surveys 2 (S2, N=6670) and 3 (S3, N=4537), average values of 4.90 (maximum of 30.23 ng m^{-3}) and 6.65 ng m^{-3} (maximum of 25.03 ng m^{-3}) were detected, respectively. High concentrations of GEM in S2 were due to the presence of an asphalt plant in the mobile transect; on the other hand, S3 was mainly affected by commercial areas and urban parks, and the elevated maximum GEM values were probably due to heavy traffic conditions. Residential and marginal areas were crossed during survey 4 (S4, N=5751), and average GEM values of 5.32±2.23 ng m^{-3} (maximum of 21.52 ng m^{-3}) were recorded. Finally, mobile survey 5 (S5, N=3516), which registered an average GEM value of 5.53±2.19 ng m^{-3} (maximum of 18.45 ng m^{-3}), was mainly conducted through residential and commercial areas. In this study, the average GEM concentrations decreased in the following order: S3>S1>S5>S4>S2. According to the frequency of GEM concentrations (Fig. 2a) measured during surveys, the log-normal distribution pattern shows the highest prevalence of 12.25%, which corresponds to a 3.92 ng m^{-3} concentration.

The average GEM concentration reported in this study, considering all surveys conducted in Mexico City,

Table 1 Summary statistics for GEM concentrations (ng m^{-3}) of different surveys realized in Mexico City

	Sampling day	N	Mean	Min	Max	Median	SD
Survey 1	31/03/2021	6652	5.62	0.31	18.30	5.34	2.03
Survey 2	17/04/2021	6670	4.90	0.24	30.23	4.57	1.79
Survey 3	08/05/2021	4537	6.65	0.27	25.03	5.93	3.27
Survey 4	09/05/2021	5751	5.32	0.30	21.52	4.88	2.23
Survey 5	27/06/2021	3516	5.53	0.20	18.45	5.13	2.19
All Data	/	27126	5.60	0.20	30.23	5.08	2.33

N number of determinations, *SD* standard deviation

was much higher (varying between 3.2 and 3.7 times higher) than background levels measured in the Northern Hemisphere (1.5–1.7 ng m^{-3}; Sprovieri et al., 2016). Globally, GEM background measurements are based on GMOS ground-based network stations. Gay et al. (2013) reported a median GEM concentration in Northern America of approximately 1.4 ng m^{-3}, approximately 3.6 times lower than our measurement. Currently, there are no data available for national Hg background values due to the scarcity of published works focusing on atmospheric measurements and the absence of a national environmental GEM monitoring network. However, comparing the average GEM value of this study with the background value calculated by Morton-Bermea et al. (2021b), the average concentration measured in this study was 2.3 times higher.

Table 2 presents a comparative list of GEM concentrations in different environments (urban, rural, mining, and industrial) from other sites around the world. Compared to the GEM concentrations in urban areas worldwide, such as in Hefei, China (2.58 ng m^{-3}; Yue et al., 2021), Tokai-mura, Japan (3.78 ng m^{-3}; Osawa et al., 2007), and Dexter, USA (1.60 ng m^{-3}; Liu et al., 2010), the GEM values reported in this work were slightly higher. Chen et al. (2013) and Seo et al. (2016) measured the total gaseous mercury (TGM) in Guangzhou,

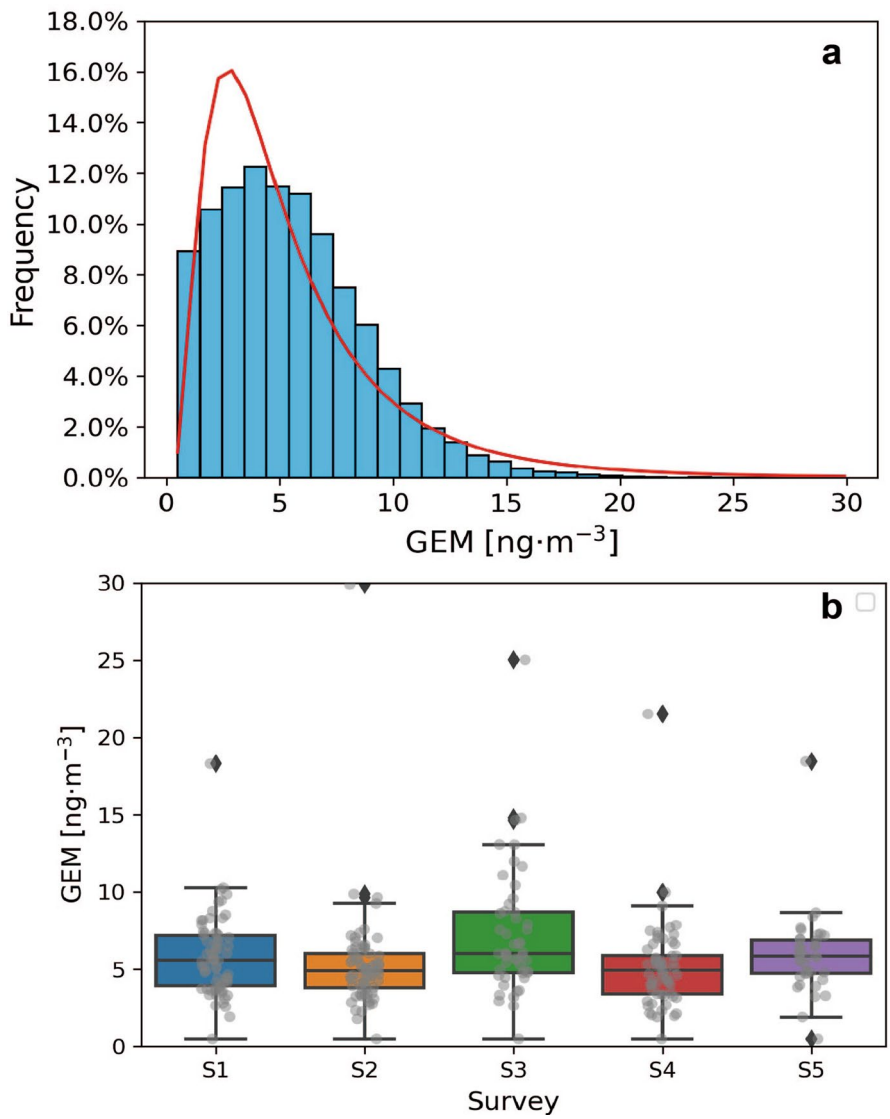

Fig. 2 (**a**) Frequency histogram of GEM distribution for the sampling periods in Mexico City. (**b**) The box plots of the GEM concentrations in several surveys over Mexico City

China, and Pohang, Korea, and reported concentrations of 4.60 and 5.17 ng m^{-3}, respectively. GEM concentrations in Mexico City have decreased by approximately 22.2% over the years, according to data published by Rutter et al. (2009). Nevertheless, in agreement with data reported in 2019 and 2020 (Morton-Bermea et al., 2021b), the concentration of atmospheric Hg in 2021 will increase by 21.1%. The average GEM concentration recorded in Mexico City was significantly higher than the values observed in rural areas, such as in Balfour, South Africa (1.99 ng m^{-3}; Beleile et al., 2019), Kodaikanal, India (1.53 ng m^{-3}; Karthik et al., 2017), and Mt. Ailaoshan, China (2.09 ng m^{-3}; Zhang et al., 2016), which are likely without Hg pollution. In addition, coastal (1.60 ng m^{-3}; Faïn et al., 2009) and volcanic (2.11 ng m^{-3}; Schiavo et al., 2020b) areas showed lower average GEM concentrations than the urban environment of Mexico City. Generally, in rural and coastal zones, atmospheric Hg levels are low due to the lack of local contamination. High GEM values, compared with those of cities, were found in industrial areas, with concentrations ranging between 2.4 (Luo et al., 2021) and 229 ng m^{-3} (Esbrí et al., 2014). The average GEM concentrations found in the mining areas of Mt. Amiata, Italy (325 ng m^{-3}; Vaselli et al., 2013) and Almaden, Spain (311.65 ng m^{-3}; Higueras et al., 2013) were even higher than those reported for industrial and urban areas affected by Hg pollution. Figure S3 shows the spatial distribution of GEM concentrations recorded in Mexico City during surveys conducted from March to June 2021. High GEM values (> 8 ng m^{-3}) were detected at several spots located in industrial areas in the north. Moreover, higher GEM levels were detected in proximity to large roads with heavy traffic compared to residential and marginal areas of the city. Nevertheless, lower GEM concentrations between 0 and 8 ng m^{-3} were most abundant and were widely distributed in the Mexico City area. Meteorological conditions, such as WS and WD, could influence the variations and spatial distributions of atmospheric GEM. Overall, the spatial variation for GEM pollution in Mexico City over the sampling period indicated that industrial areas and heavy traffic roads are the dominant local sources of GEM.

Daily variation of GEM and comparison with criteria pollutant concentrations

Figure 2b shows a statistical boxplot with GEM results in different surveys of warm, dry periods in Mexico

Table 2 Comparison of average GEM concentrations (ng m^{-3}) presented in this study and values reported at different locations worldwide

Location	Sample site	Monitoring period	GEM	Reference
Mexico city, Mexico	Urban	Mar 31, Apr 17, May 8 and 9, and June 27, 2021	5.60	This study
Hefei, China	Urban	Mar to May, 2016	2.58	Yue et al. (2021)
Tokai-mura, Japan	Urban	Oct 2005 to Sept 2006	3.78	Osawa et al. (2007)
Dexter, USA	Urban	1 year (2004)	1.60	Liu et al. (2010)
*Guangzhou, China	Urban	Nov 2010 to Oct 2011	4.60	Chen et al. (2013)
*Pohang, Korea	Urban	2 years (2012 to 2013)	5.0	Seo et al. (2016)
Mexico City, Mexico	Urban	March 9–25, 2006	7.20	Rutter et al. (2009)
Mexico City, Mexico	Urban	May 12, 2019, and May 22, 2020	4.42	Morton-Bermea et al. (2021b)
*Kodaikanal, India	Rural	Nov 2012 to Sept 2013	1.53	Karthik et al. (2017)
*Balfour, South Africa	Rural	1 year (2009)	1.99	Beleile et al. (2019)
Popocatépetl, Mexico	Volcanic/rural	March 28, 2019	2.11	Schiavo et al. (2020b)
Colorado, USA	Coastal/rural	Apr 28 to July 1, 2008	1.60	Faïn et al. (2009)
Mt. Ailaoshan, China	Rural	May 2011 to May 2012	2.09	Zhang et al. (2016)
Zhongshan, China	Polluted/industry	July 29 to August 10, 2019	2.4	Luo et al. (2021)
Mt. Amiata, Italy	Polluted/mining	May, 2011	325	Vaselli et al. (2013)
Almaden, Spain	Polluted/mining	March and June 2002	311.65	Higueras et al. (2013)
Flix, Spain	Polluted/industry	Between 2007 and 2012	229	Esbrí et al. (2014)

*Atmospheric total gaseous mercury (TGM)

City. A clear difference is observed between GEM recovery in commercial and residential areas (S2, S4, and S5) compared to industrial and high traffic areas (S1 and S3). The average GEM concentrations in S1 and S3 were 1.25 to 12.5% and 16.8 to 26.3%, respectively, higher than those in the other surveys (*t* test, $p < 0.001$). On the other hand, the median values did not change significantly between surveys. Anomalous values of GEM (boxplot outliers) were present in all mobile transect samples. An outlier with maximum GEM values was recognized in S2 because it passes close to the asphalt plant (Spreadbury et al., 2021) situated in the south of the city.

Daily time series for GEM average values, pollutant criteria, and meteorological parameters (Table 3) during our observation periods are shown (Fig. 3). Three correlation events involving GEM and trace gases occurred in Mexico City during S1, S4, and S5. In S1 and S4, levels of GEM, PM_x ($PM_{2.5}$ and PM_{10}), trace gases (NO_2, SO_2, and CO), and T increased significantly and showed similar temporal variation trends. On the other hand, correlations characterized by significant decreases occurred in S5 and involved trace gases, PM_x, and T. The decreases in concentrations were probably caused by unfavorable climatic conditions on the sampling day, which was characterized by light rain and cloudy skies. The predominant phenomenon operating under these conditions is wet deposition, which "cleans" the air by removing pollutants (e.g., sulfate and nitrate aerosols). The CO level in S1 was the only case for which the trend was the opposite of those for other trace gases and PM_x. Correlations were more evident in periods with lower WS, which resulted in less dilution of GEM and trace gases in the atmosphere. No apparent correlations were found during S2, which may be due to adverse weather conditions (e.g., high WS), which precluded detection of coincidences between GEM, trace gases, and PM_x, or the absence of fixed measurement stations near the survey transect.

Table 4 shows daily Spearman correlation (p value < 0.05) coefficients among GEM and other atmospheric pollutants. Significant correlations were found between GEM, $PM_{2.5}$, NO_2, and SO_2. The correlations between GEM and NO_2 in S1 ($r=0.95$), S3 ($r=0.74$), S4 ($r=0.88$), and S5 ($r=0.99$) were significant compared to that in S2 ($r=-0.67$, p value > 0.05). GEM and SO_2 were significantly correlated in S1 ($r=0.95$), S3 ($r=0.84$), S4 ($r=0.98$), and S5 ($r=0.84$); in contrast, in S2, the p value was > 0.05 ($r=0.36$). The primary source of NO_2 and SO_2 in an urban environment and of relatively low-concentration GEM is motor vehicle exhaust emissions. GEM emissions from soil could contribute to atmospheric contamination in periods of intense solar radiation (Esbrí et al., 2016). In S4, a significant correlation was found between $PM_{2.5}$ and GEM ($r=0.90$). A high concentration for $PM_{2.5}$ was recorded in S4 at the crossway with the Mexico City

Table 3 Average meteorological data, including climate and road traffic condition of sample days, PM_x, and trace gases for different profiles (S1–S5) carried out in pre-rainy period during 2021

Survey	S1	S2	S3	S4	S5
Date	March 31	April 17	May 8	May 9	June 27
Meteorology					
Temperature (°C)	18.90	27.15	18.46	19.37	14.93
Relative humidity (%)	27.75	16.50	47.67	52.75	72.33
Wind direction (main)	N-NW	SW	S	SE	E-SE
Wind speed ($m \cdot s^{-1}$)	1.97	3.55	2.87	1.42	1.36
Climate	Sunny	Sunny	Sunny	Cloudy	Cloudy, rainy
Traffic	Heavy	Moderate/heavy	Moderate/heavy	Moderate	Low
Trace gases					
NO_2 (ppb)	61.75	8.37	12.16	33.75	13
SO_2 (ppb)	4.37	6.50	2.16	1.25	1.34
CO (ppm)	1.20	0.31	0.14	0.77	0.38
$PM_{2.5}$ ($\mu g \cdot m^{-3}$)	45	31.05	23.34	47.25	4
PM_{10} ($\mu g \cdot m^{-3}$)	76.50	67.75	37	55.50	5.34

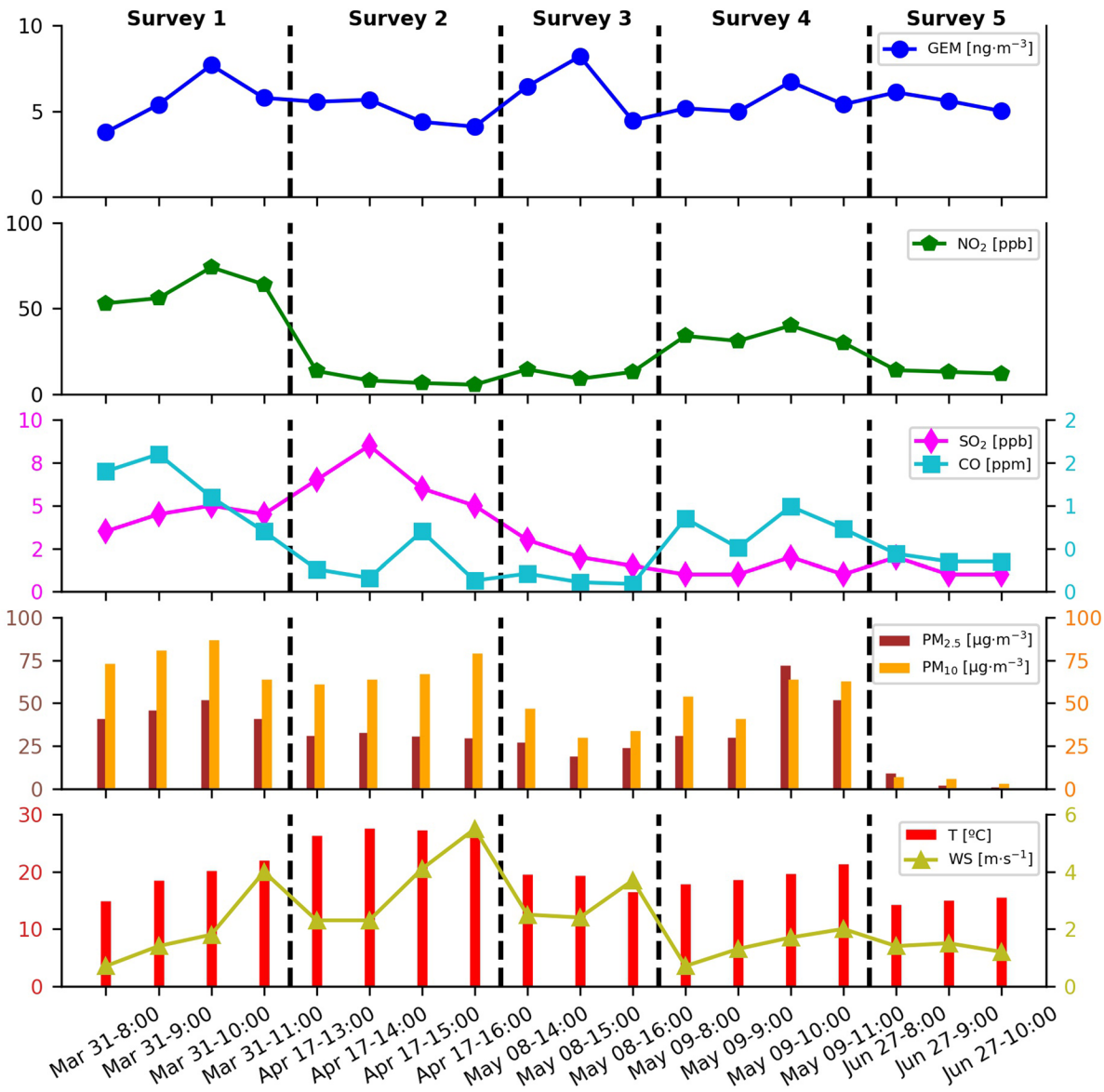

Fig. 3 The hourly average of GEM, trace gases, particulate matter (PM), and meteorological parameters during mobile survey during spring period in Mexico City

International Airport (Marisol & Harrison, 2014). Although GEM and CO usually show similar anthropogenic emission sources (e.g., wildfires, residential coal burning, and industry activity), no significant correlation was found during the measurement periods.

The accumulation of GEM in the atmosphere, combined with local anthropogenic emissions (e.g., exhaust emissions, coal fires, cement production), and moderate WS (i.e., low dilution effect), contributed to pollution and secondary aerosol formation. Secondary processes, such as photoreduction, apparently do not play important roles in GEM variation and atmosphere reduction compared to primary emissions (e.g., fossil fuel burning from vehicles). Oxidation ($Hg^0 \rightarrow Hg^{2+}$) is the crucial process that removes GEM from the atmosphere (Si & Ariya, 2018). Ozone (O_3), OH, and NO_3 radicals, as well as halogens, are chemical species that can affect Hg oxidation. Si and

Table 4 Pearson's correlation coefficients between GEM and other components, such as trace gases, PM, and meteorological parameters

GEM	S1	S2	S3	S4	S5
NO_2	0.95*	−0.67	0.74*	0.88*	0.99*
SO_2	0.95*	0.36	0.84*	0.98*	0.84*
CO	−0.39	−0.33	0.19	0.79	0.84
$PM_{2.5}$	0.83	0.88	−0.59	0.90*	0.90
PM_{10}	0.51	−0.84	−0.19	0.70	0.97
T	0.73	−0.35	0.84	0.31	−0.99
Rh	−0.72	−0.14	−0.90	−0.32	0.91
WS	0.36	−0.97	−0.91	0.44	0.69
WD	−0.034	−0.74	0.72	−0.29	0.97

*Correlation is significant at p value < 0.05

Ariya (2018) reported recent models that indicated the complexity of GEM oxidation in the atmosphere. According to models and published work, some chemical species are more effective in oxidizing Hg under certain conditions, depending on geographic location (inland and coastal site), hour of the day, and season (Gabay et al., 2020; Ye et al., 2016).

GEM source identification

Mexico City is located inside a basin and is surrounded by mountains. Celada-Murillo et al. (2013) reported that north–south winds are an important mechanism providing air exchange among cities and local human settlements, according to seasonal data collected during sampling campaigns in 2006. Surface air flows from the Pacific and the Gulf of Mexico are recognized, suggesting southwest and northeast wind directions with regional features (de Foy et al., 2005). In this study, daily variations observed on different survey days indicated that the wind blew from the N-NW (S1), SW (S2), S (S3), SE (S4), and E-SE (S5) (Fig. S4).

We used a HYSPLIT forward dispersion model to assess the relative contributions of different anthropogenic GEM emission sources over a 12-h time period, their regional and pathway transports, and possible impacts on the air quality of Mexico City (Fig. 4). Three different locations, the Miguel Hidalgo refinery, Apaxco, and Popocatépetl volcano, were added as potential GEM source contributors: (i) the Miguel Hidalgo refinery is an important industrial corridor and petroleum refinery in Central Mexico, and it has the ability to process 3×10^5 barrels of crude material per day and the objective of supplying Mexico City with refined gasoline (Sosa et al., 2013); (ii) the Apaxco area, also called a "sacrifice zone" for the local community, is an industrial corridor with cement, waste coprocessing, and thermoelectric plants, as well as refineries and agrochemical factories; and (iii) the Popocatépetl volcano is one of the most active volcanoes in the world and a large emitter of GEM into the atmosphere (Schiavo et al., 2020a). The results of simulation modeling on May 8 and 9 showed that the central and northern areas of Mexico City were influenced by air mass dispersion coming from the Tula and Apaxco industrial corridors. The other days showed dissimilar trends and dispersion of contaminants that did not affect the Mexico City area. On March 31, the trajectory of the air mass affected the western part of the study area, probably with strongly diluted GEM concentrations. In both locations, an opposite tendency was noted on June 27, with prevalent dispersion toward the north. Moreover, the results indicated that the plume of Popocatépetl volcano moderately influenced the southeastern area of Mexico City during measurement survey days, mainly on March 31 and May 8. In addition, the volcanic plume showed a preference for travel to the north on June 27, as displayed for the industrial areas. Although contamination from various sources can modify the Mexico City air quality, the GEM level is subject to strong dilution in the atmosphere, which produces a decrease in concentration. At this point, local sources are more effective for GEM pollution than regional transport. The lack of important regional transport is confirmed by the absence of a significant correlation between GEM and CO. Weiss-Penzias et al. (2006) and Wang et al. (2021) indicated strong regional transport when GEM and CO correlations were recognized, considering the long atmospheric lifetimes and similar sources exhibited by both contaminants.

Local sources of GEM in urban environments are mainly characterized by (i) motor vehicle exhaust emissions, (ii) cement production, and (iii) municipal solid waste (MSW), including electronic waste (e-waste). Won et al. (2007) and Landis et al. (2007) demonstrated pollution by elemental Hg from fuel, i.e., gasoline, diesel, and liquefied petroleum gas (LPG), and the largest content of Hg was found in LPG, followed by gasoline and diesel. An automobile

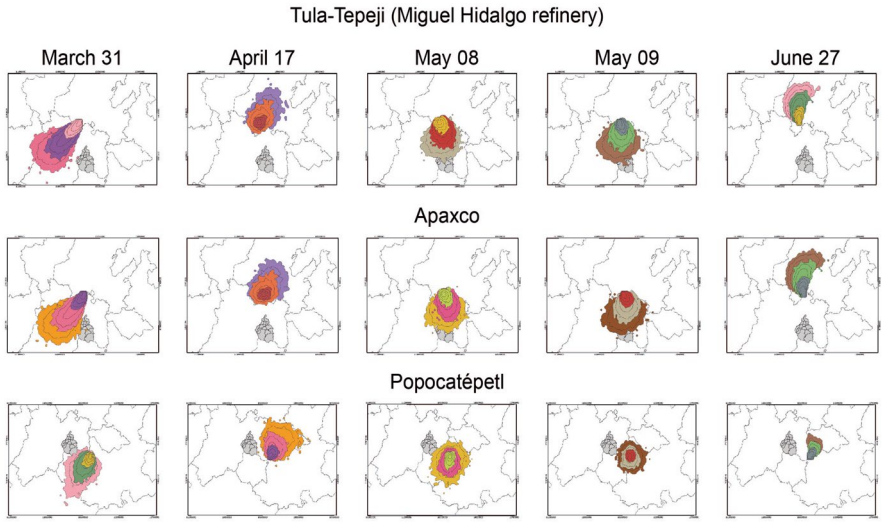

Fig. 4 HYSPLIT forward dispersion model simulation of the air mass from three sites, Miguel Hidalgo refinery, Apaxco industrial complex, and Popocatépetl volcano, which could contribute to GEM air pollution in Mexico City (solid gray)

could emit concentrations of GEM between 1.5 and 27 ng m^{-3} into the atmosphere during idling and driving (Won et al., 2007). GEM contents were also analyzed and detected in several vehicle parts and additives, such as brake rotors and pads, engine coolant, and lubricating oil (Hoyer et al., 2004). Studies focused on removing GEM from exhaust emissions have been varied (e.g., Presto & Granite, 2006; Yang et al., 2007). Currently, removal of mercury from the exhaust gases of combustion vehicles is not effective and is based entirely on the limited ability of some compounds, such as sulfur and halogens, to oxidize mercury. Wdowin et al. (2014) reported effective use of activated carbon and synthetic zeolite (with impregnated silver) to capture mercury from exhaust emissions. The cement industry is classified as one of the principal emitters of GEM (Fukuzaki et al., 1986). In 2010, it was estimated that China discharged approximately 100 tons of GEM into the atmosphere (Zhang et al., 2015). Hg is vaporized at high temperature during clinker cement production, a long and complicated procedure called the "precalciner process" that includes heating and decomposing raw material and roasting with coal in a rotary kiln system (Wang et al., 2016). Kogut et al. (2021) reiterated the importance of reducing mercury vapors from cement production. GEM removal from the cement process can be done through (i) understanding the Hg distribution in each process step and (ii) using absorption methods such as activated charcoal, selective catalytic reduction (SCR), and selective noncatalytic reduction (SNCR). In an urban environment, MSW, which is toxic and dangerous to humans, contributes to air, soil, and water pollution by heavy metals (Akinwumi et al., 2018; Ostad-Ali-Askari et al., 2017). Waste control and management, based on governmental and academic perspectives, are essential to prevent serious consequences for the environment (Kebede et al., 2021). E-waste contamination has increased in the last decade. In recent years, incineration of e-waste has generated large amounts of particulates, heavy metals, and GEM released into the atmosphere. Decharat (2018) investigated GEM levels resulting from urination by e-waste shop workers and found airborne concentrations above 29.000 ng m^{-3} and reported symptoms of headaches, insomnia, and weakness. With the growing demand for electronic components worldwide, the disposal of electronic waste is a priority human health problem.

GEM health risk assessment

The World Health Organization (WHO) suggested an average annual GEM exposure of 1000 ng m^{-3} (HQ $\approx$ 3) in air quality guidelines (WHO, 2000). Furthermore, the WHO (WHO, 2003) indicated maximum daily exposures to GEM concentrations of approximately 200 ng m^{-3} (HQ $\approx$ 0.6) by considering a typical workweek (8 h/day and 5 days/week). Occupational GEM inhalation limits, established at

40 ng m^{-3} (HQ ≈ 0.1), were proposed by the Japan Ministry of the Environment based on minimization of adverse chronic effects in the exposed population (MOE (Ministry of the Environment), 2003). We determined the average and standard deviation for sample GEM concentrations measured during the five surveys of Mexico City. Our average GEM concentrations were significantly lower than the limits fixed by the WHO. Instead, in considering the maximum GEM values recorded in this study, the concentrations were similar to the inhalation limits reported by the Japanese government (MOE, 2003) for occupational exposure.

The noncarcinogenic human health risk of GEM based on HQ (Table 5) was evaluated for the general population (adults and children) by using the inhalation exposure route, as indicated in the "Health risk assessment" section. Inhalation of GEM vapor, which is characterized by high pressures at ambient temperature, is the major route for exposure of the human body. The GEM risks (HQ) registered during the surveys decreased in the order S3 (2.12E−02) > S1 (1.80E−02) > S5 (1.77E−02) > S4 (1.70E−02) > S2 (1.57E−02). The average HQ value for the entire study area was 1.79E-02 ± 1.10E−03. The HQ values reported in this work did not exceed the no-risk level, i.e., HQ > 1. The probabilistic values for different inhalation HQ percentiles (Q0 to Q4) are listed in Table S2. The HQ values calculated for the various percentiles do not present health risks, according to the USEPA model (USEPA, 2011). The 25th, 50th, and 75th percentiles were 9.62E−03, 4.84E−02, and 2.42E−02, respectively, showing HQ values similar to those reported in Table 5 (≈1E−02). The 99.9th percentile HQs were 0.28 and 0.35 in S1 and S3, respectively.

Based on the levels of GEM concentrations and HQ risks evaluated in Mexico City, it is expected that people living close to high traffic roads and in the northern area are more prone to possible public health complications arising from long-term acute exposure. The assessment discussed in this work only reports average GEM exposure. Even after considering that Hg vapors are very dangerous and almost totally absorbed by the human body, another pathway, ingestion through dust (e.g., urban or soil), food, and water, must be subject to accumulated risk calculations (hazard index).

Table 5 Health risk assessment of GEM in Mexico City during pre-rainy period, 2021

Survey	CEC_{Hg} (ng m^{-3})	HQ	HQ SD
S1	5.39	1.80E−02	9.68E−03
S2	4.70	1.57E−02	8.92E−03
S3	6.37	2.12E−02	1.36E−03
S4	5.10	1.70E−02	1.03E−03
S5	5.30	1.77E−02	1.02E−03
Average	5.37	1.79E−02	1.10E−03

HQ SD, HQ standard deviation

Limitations

This study has the following limitations:

1. We carried out surveys, and fixed air quality stations were used to provide comparisons with other trace gases, particulates, and meteorological parameters. It was not possible to complement the surveys with mobile instruments for detection of other trace gases. Moreover, comparisons among various compounds could be made by taking into consideration hourly averages, as reported by RAMA stations. However, considering the limited amount of daily GEM data, comparing concentrations every 15 min would have been preferable.
2. GEM is highly diluted by contact with the atmosphere. In urban environments, it is important to find areas or specific points with anomalous concentrations of GEM and place fixed measurement stations operating for certain periods of time to evaluate daily, monthly, and seasonal variations.
3. Many studies have reported variations in Hg levels over seasons and in pre- and post-monsoon periods (Luo et al., 2021; Yue et al., Yuan et al., 2021). We investigated GEM concentrations around Mexico City only during the pre-rainy period (spring season) with the objective of finding specific areas characterized by anomalous concentrations. As reported by Retama et al. (2015), the concentrations of pollutants in Mexico City are significantly elevated during the cold-dry period (spring season) compared to the rainy and warm-dry periods.

Conclusion

This study investigated the outdoor atmospheric characteristics, spatiotemporal variations, and potential sources of GEM in Mexico City during the spring season of 2021. Various mobile transects were carried out around the city to measure the concentration of GEM in real time. The results showed that the recorded average GEM concentrations, which ranged from 5.23 to 6.65 ng m^{-3}, were similar over the measurement campaign. The major differences were found by comparing the maximum values between surveys. Anomalous emission points were registered in S2 (30.23 ng m^{-3}) and S3 (25.03 ng m^{-3}) while passing through an industrial area and high traffic road, respectively. Overall, the GEM concentration was approximately 2.3–3.7 times higher than that in the Northern Hemisphere (1.5–1.7 ng m^{-3}) and local background (2.53 ng m^{-3}). Compared with the 2006–2007 period, GEM concentration shows a decrease of 22.2%; on the other hand, an increase of 21.7% was registered in comparison with a period of 2020. The year of 2020 was characterized by lockdown due to the recent SARS-CoV-2 pandemic and a decrease of anthropogenic emissions. Actually, no air quality and Hg emissions control policy has been implemented by the Mexican Central Government. The relationship between GEM, criteria pollutants, and meteorological parameters has been studied. The significative correlation (t test, $p < 0.05$) was found with SO_2, NO_2, and $PM_{2.5}$. Considering temperature and solar radiation, a close relationship was found between these parameters and Hg emissions.

Forward dispersion simulation models showed that GEM regional transport affects only the relative contamination of Mexico City, especially after considering strong GEM dilution in the atmosphere. However, the areas most affected by the dispersion of contaminants from Tula and Apaxco are the northern and western zones. Although considered one of the largest GEM emitters, Popocatépetl volcano does not contribute to contamination in this particular season with these climate conditions. According to the study, the main source of GEM in the city is local pollution, including that caused by industrial activity, cement production, MSW (including e-waste and fluorescent lamp), and fossil fuel combustion.

The results of the health risk assessment indicated that the general population living in the area of Mexico City has no carcinogenic risk for GEM exposure by inhalation. The GEM concentrations reported in this work are within the limits established by the USEPA and WHO. This demonstrated that adverse health effects can appear after prolonged GEM exposure, even at low concentrations. It is recommended that GEM emissions from fossil sources (gasoline and diesel) should be substantially reduced, and the management of waste, mainly in urban environments, should be improved.

Acknowledgements Lumex RA-915 M mercury analyzer was purchased with the financial support of the Project 268074 GEMEX. The authors acknowledge the NOAA Air Resources Laboratory (ARL) for the provision of the HYSPLIT model and RAMA network for providing data used in this publication.

Availability of data and material The datasets collected and used during the current study are available on reasonable request.

Declarations

Conflict of interest The authors declare no competing interests.

References

Angot, H., Dastoor, A., De Simone, F., Gårdfeldt, K., Gencarelli, C. N., Hedgecock, I. M., Langer, S., Magand, O., Mastromonaco, M. N., Nordstrøm, C., Pfaffhuber, K. A., Pirrone, N., Ryjkov, A., Selin, N. E., Skov, H., Song, S., Sprovieri, F., Steffen, A., Toyota, K., … Dommergue, A. (2016). Chemical cycling and deposition of atmospheric mercury in polar regions: Review of recent measurements and comparison with models. *Atmospheric Chemistry and Physics, 16*, 10735–10763. https://doi.org/10.5194/acp-16-10735-2016

Akinwumi, I. I., Booth, C. A., Ojuri, O. O., Ogbiye, A. S., & Coker, A. O. (2018). Chapter: Containment of pollution from urban waste disposal sites. *Book: Urban pollution: Science and Management*. https://doi.org/10.1002/9781119260493.ch17

Bjørklund, G., Dadar, M., Mutter, J., & Aaseth, J. (2017). The toxicology of mercury: Current research and emerging trends. *Environmental Research, 159*, 545–554. https://doi.org/10.1016/j.envres.2017.08.051

Bank, M. S. (2020). The mercury science-policy interface: History, evolution and progress of the Minamata Convention. *Science of the Total Environment, 722*, 137832. https://doi.org/10.1016/j.scitotenv.2020.137832

Bargagli, R. (2016). Atmospheric chemistry of mercury in Antarctica and the role of cryptogams to assess deposition patterns in coastal ice-free areas. *Chemosphere, 163*, 202–208. https://doi.org/10.1016/j.chemosphere.2016.08.007

Beleile, M. D., Piketh, S. J., Burger, R. P., Venter, A. D., & Naidoo, M. (2019). Characterization of ambient total

gaseous mercury concentrations over the South African Highveld. *Atmospheric Pollution Research, 10*, 12–23. https://doi.org/10.1016/j.apr.2018.06.001

Berlin, M., Zalups, R. K., & Fowler, B. A. (2015). Mercury. In G. F. Nordber, B. A. Fowler, & M. Nordberg (Eds.), *Handbook on the toxicology of metals, Specific metals II (fourth ed.)* (pp. 1013–1075). Academic Press, Amsterdam (2015). https://doi.org/10.1016/B978-0-444-59453-2.00046-9

Bose-O'Reilly, S., Lettmeier, B., Gothe-Matteucci, R., Beinhoff, C., Siebert, U., & Drasch, G. (2008). Mercury as a serious health hazard for children in gold mining areas. *Environmental Research, 107*, 89–97. https://doi.org/10.1016/j.envres.2008.01.009

Budnik, L. T., & Casteleyn, L. (2019). Mercury pollution in modern times and its socio-medical consequences. *Science of the Total Environment, 654*, 720–734. https://doi.org/10.1016/j.scitotenv.2018.10.408

Celada-Murillo, A-T., Carreón-Sierra, S., Salcido, A., Castro, T., Peralta, O., & Georgiadis, T. (2013). Main characteristics of Mexico City local wind events during the MILAGRO 2006 campaign within a meso-β scale lattice wind modeling approach. *International Scholarly Research Notices, 2013*(605210), 14. https://doi.org/10.1155/2013/605210

Chen, L., Liu, M., Xu, Z., Fan, R., Tao, J., Chen, D., Zhang, D., Xie, D., & Sun, J. (2013). Variation trends and influencing factors of total gaseous mercury in the Pearl River Delta—A highly industrialized region in South China influenced by seasonal monsoons. *Atmospheric Environment, 77*, 757–766. https://doi.org/10.1016/j.atmosenv.2013.05.053

Cizdziel, J. V., Jiang, Y., Nallamothu, D., Brewer, J. S., & Gao, Z. (2019). Air/surface exchange of gaseous elemental mercury at different landscapes in Mississippi, USA. *Atmosphere, 10*(9), 538. https://doi.org/10.3390/atmos10090538

Decharat, S. (2018). Urinary mercury levels among workers in e-waste shops in Nakhon Si Thammarat Province, Thailand. *Journal of Preventive Medicine & Public Health, 51*(4), 196–204. https://doi.org/10.3961/jpmph.18.049

de Foy, B., Caetano, E., Magaña, V., Zitácuaro, A., Cárdenas, B., Retama, A., Ramos, R., Molina, L. T., & Molina, M. J. (2005). Mexico City basin wind circulation during the MCMA-2003 field campaign. *Atmospheric Chemistry and Physics, 5*, 2267–2288. https://doi.org/10.5194/acp-5-2267-2005

De la Rosa, D. A., Volke-Sepúlveda, T., Solórzano, G., Green, C., Tordon, R., & Beauchamp, S. (2004). Survey of atmospheric total gaseous mercury in Mexico. *Atmospheric Environment, 38*, 4839–4846. https://doi.org/10.1016/j.atmosenv.2004.06.013

De la Rosa, D. A., Velasco, A., Rosas, A., & Volke-Sepúlveda, T. (2006). Total gaseous mercury and volatile organic compounds measurements at five municipal solid waste disposal sites surrounding the Mexico City Metropolitan Area. *Atmospheric Environment, 40*, 2079–2088. https://doi.org/10.1016/j.atmosenv.2005.11.055

dos Santos, A.A., Hort, M.A., Culbreth, M., López-Granero, C., Farina, M., Rocha, J.B.T., Aschner, M. (2016). Methylmercury and brain development: A review of recent literature. *Journal of Trace Elements in Medicine and Biology*, *38*, 99–107.

Draxler, R. (2008). NOAA - Air resources laboratory - FAQ - How do i estimate the absolute (in km) and relative (%) errors when using the HYSPLIT trajectory model?. https://www.ready.noaa.gov/HYSPLIT.php

Edwards, B. A., Kushner, D. S., Outridge, P. M., Wang, F. (2021). Fifty years of volcanic mercury emission research: Knowledge gaps and future directions. *Science of The Total Environment*, *757*, 143800. https://doi.org/10.1016/j.scitotenv.2020.143800

Esbrí, J. M., López-Berdonces, M. A., Fernández-Calderón, S., Higueras, P., & Díez, S. (2014). Atmospheric mercury pollution around a chlor-alkali plant in Flix (NE Spain): An integrated analysis. *Environmental Science and Pollution Research, 22*, 4842–4850. https://doi.org/10.1007/s11356-014-3305-x

Esbrí, J. M., Martínez-Coronado, A., & Higueras, P. L. (2016). Temporal variations in gaseous elemental mercury concentrations at a contaminated site: Main factors affecting nocturnal maxima in daily cycles. *Atmospheric Environment, 125*, 8–14. https://doi.org/10.1016/j.atmosenv.2015.10.064

Esdaile, L. J., & Chalker, J. M. (2018). The mercury problem in artisanal and small-scale gold mining. *Chemistry, A European Journal, 24*, 6905–6916. https://doi.org/10.1002/chem.201704840

Estrada, F., Martínez-Arroyo, A., Fernández-Eguiarte, A., Luyando, E., & Gay, C. (2009). Defining climate zones in México City using multivariate analysis. *Atmósfera, 22*(2), 175–193. https://www.revistascca.unam.mx/atm/index.php/atm/article/view/8625

Faïn, X., Obrist, D., Hallar, A. G., Mccubbin, I., & Rahn, T. (2009). High levels of reactive gaseous mercury observed at a high elevation research laboratory in the Rocky Mountains. *Atmospheric Chemistry and Physics, 9*, 8049–8060. https://doi.org/10.5194/acp-9-8049-2009

Fuentes García, G., Bravo Álvarez, H., Sosa Echeverría, R., Rosas de Alba, S., Magaña Rueda, V., Caetano Dosantos, E., & Vázquez Cruz, G. (2017). Spatial and temporal variability of atmospheric mercury concentrations emitted from a coal-fired power plant in Mexico. *Journal of the Air & Waste Management Association, 67*, 973–985. https://doi.org/10.1080/10962247.2017.1314871

Fukuzaki, N., Tamura, R., Hirano, Y., & Mizushima, Y. (1986). Mercury emission from a cement factory and its influence on the environment. *Atmospheric Environment, 20*, 2291–2299. https://doi.org/10.1016/0004-6981(86)90059-4

Gabay, M., Raveh-Rubin, S., Peleg, M., Fredj, E., & Tas, E. (2020). Is oxidation of atmospheric mercury controlled by different mechanisms in the polluted continental boundary layer vs. remote marine boundary layer?. *Environmental Research Letters, 15*(6), 064026. https://doi.org/10.1088/1748-9326/ab7b26

García-Martínez, R., Hernández-Silva, G., Pavia-Hernández, R., Schiavo, B., Flores-Espinosa, M., Wellens, A., Torres-Jardon, R., Garcia-Reynoso, A., Martínez-Arroyo, A., Gavilán-García, A., & Ruíz-Suárez, L. G. (2021). Total gaseous mercury levels in the vicinity of the central Mexico mountain mining zone and its dispersion area. *Air*

Quality, Atmosphere & Health. https://doi.org/10.1007/s11869-021-01068-w

Gay, D. A., Schmeltz, D., Prestbo, E., Olson, M., Sharac, T., & Tordon, R. (2013). The Atmospheric Mercury Network: Measurement and initial examination of an ongoing atmospheric mercury record across North America. *Atmospheric Chemistry and Physics, 13*, 11339–11349. https://doi.org/10.5194/acp-13-11339-2013

Gibb, H., & O'Leary, K. G. (2014) Mercury Exposure and Health Impacts among Individuals in the Artisanal and Small-Scale Gold Mining Community: A Comprehensive Review. *Environmental Health Perspectives*, *122*, 667–672. https://doi.org/10.1289/ehp.1307864

Gyamfi, O., Sorenson, P. B., Darki, G., Ansah, E., & Bak, J. L. (2020). Human Health risk assessment of exposure to indoor mercury vapor in a Ghanaian artisanal small-scale gold mining community. *Chemosphere, 241*, 125014. https://doi.org/10.1016/j.chemosphere.2019.125014

Gustin, M. S. (2003). Are mercury emissions from geologic sources significant? A status report. *Science of the Total Environment, 304*, 153–167. https://doi.org/10.1016/S0048-9697(02)00565-X

Gustin, M. S., Amos, H. M., Huang, J., Miller, M. B., & Heidecorn, K. (2015). Measuring and modeling mercury in the atmosphere: A critical review. *Atmospheric Chemistry and Physics, 15*, 5697–5713. https://doi.org/10.5194/acp-15-5697-2015

Gustin, M. S., Bank, M. S., Bishop, K., Bowman, K., Brafireun, B., Chételat, J., Eckley, C. S., Hammerschmidt, C. R., Lamborg, C., Lyman, S., Martínez-Cortizas, A., Sommar, J., Tsz-Ki Tsui, M., & Zhang, T. (2020). Mercury biogeochemical cycling: A synthesis of recent scientific advances. *Science of the Total Environment, 737*, 139619. https://doi.org/10.1016/j.scitotenv.2020.139619

Gworek, B., Dmuchowski, W., Baczewska, A. H., Bragoszewska, P., Bemowska-Kalabun, O., & Wrzosek-Jakubowska, J. (2017). Air contamination by mercury, emissions and transformations – A review. *Water, Air, & Soil Pollution, 228*, 123. https://doi.org/10.1007/s11270-017-3311-y

Heidari-Beni, M., Golshahi, J., Esmaillzadeh, A., & Azadbakht, L. (2015). Potato consumption as high glycemic index food, blood pressure, and body mass index among Iranian adolescent girls. *ARYA Atheroscler, 11*(Suppl 1), 81–87.

Higueras, P., Esbrí, J. M., Oyarzun, R., Lillo, J., Llanos, W., Martínez-Coronado, A., Lillo, J., López-Berdonces, M. A., & García-Noguero, E. M. (2013). Industrial and natural sources of gaseous elemental mercury in the Almadén district (Spain): An updated report on this issue after the ceasing of mining and metallurgical activities in 2003 and major land reclamation works. *Environmental Research, 125*, 197–208. https://doi.org/10.1016/j.envres.2012.10.011

Hintelmann, H. (2010). Organomercurials: Their formation and pathways in the environment. *Royal Society of Chemistry, 7*, 365–401. https://doi.org/10.1039/9781849730822-00365

Hoyer, M., Baldauf, R. W., Scarbro, C., Barres, J., & Keeler, G. J. (2004). Mercury Emissions from Motor Vehicles. *USEPA government*. http://citeseerx.ist.psu.edu/viewdoc/download?doi=10.1.1.508.4571r&rep=rep1&type=pdf

Hylander, L. D., & Goodsite, M. E. (2005). Environmental costs of the mercury pollution. *Science of the Total Environment, 368*, 352–370. https://doi.org/10.1016/j.scitotenv.2005.11.029

INEGI. (2020). Censo de Población y Vivienda 2020. Instituto Nacional de Estadística y Geografía.https://www.inegi.org.mx/contenidos/productos/prod_serv/contenidos/espanol/bvinegi/productos/nueva_estruc/702825198701.pdf

Karthik, R., Paneerselvam, A., Ganguly, D., Hariharan, G., Srinivasalu, S., Purvaja, R., & Ramesh, R. (2017). Temporal variability of atmospheric total gaseous mercury and its correlation with meteorological parameters at a high-altitude station of the South India. *Atmospheric Pollution Research, 8*, 173. https://doi.org/10.1016/j.apr.2016.08.010

Kebede, Y. S., Alene, M. M. A., & Endalemaw, N. T. (2021). Urban landfill investigation for managing the negative impact of solid waste on environment using geospatial technique. A case study of Assosa town, Ethiopia. *Environmental Challenges, 4*, 100103. https://doi.org/10.1016/j.envc.2021.100103

Kim, H. S., Kim, Y. J., & Seo, Y. R. (2015). An overview of carcinogenic heavy metal: Molecular toxicity mechanism and prevention. *Journal of Cancer Prevention, 20*(4), 232–240. https://doi.org/10.15430/JCP.2015.20.4.232

Kogut, K., Górecki, J., & Burmistrz, P. (2021). Opportunities for reducing mercury emissions in the cement industry. *Journal of Cleaner Production, 293*, 126053. https://doi.org/10.1016/j.jclepro.2021.126053

Landis, M. S., Lewis, C. W., Stevens, R. K., Keeler, G. J., Dvonch, J. T., & Tremblay, R. T. (2007). Ft. McHenry tunnel study: Source profiles and mercury emissions from diesel and gasoline powered vehicles. *Atmospheric Environment, 41*, 8711–8724. https://doi.org/10.1016/j.atmosenv.2007.07.028

Li, F., Ma, C., & Zhang, P. (2020). Mercury deposition, climate change and anthropogenic activities: A review. *Frontiers in Earth Science*. https://doi.org/10.3389/feart.2020.00316

Liu, B., Keeler, G. J., Dvonch, J. T., Barres, J. A., Lynam, M. M., Marsik, F. J., & Morgan, J. T. (2010). Urban-rural differences in atmospheric mercury speciation. *Atmospheric Environment, 44*, 2013–2023. https://doi.org/10.1016/j.atmosenv.2010.02.012

Lindberg, S., Bullock, R., Ebinghaus, R., Engstrom, D., Feng, X., Fitzgerald, W., Pirrone, N., Prestbo, E., & Seigneur, C. (2007). A synthesis of progress and uncertainties in attributing the sources of mercury in deposition, AMBIO. *A Journal of the Human Environment*, *36*(1), 19–33. https://doi.org/10.1579/0044-7447(2007)36[19:ASOPAU]2.0.CO;2

Lyman, S. N., Cheng, I., Gratz, L. E., Weiss-Penzias, P., & Zhang, L. (2020). An updated review of atmospheric mercury. *Science of the Total Environment, 707*, 135575. https://doi.org/10.1016/j.scitotenv.2019.135575

Luo, Q., Ren, Y., Sun, Z., Li, Y., Yang, S., Zhang, W., Hu, Y., & Cheng, H. (2021). Atmospheric mercury pollution caused by fluorescent lamp manufacturing and the associated human health risk in a large industrial and commercial city. *Environmental Pollution, 269*, 146. https://doi.org/10.1016/j.envpol.2020.116146

Marisol, M., & Harrison, R. M. (2014). Aircraft engine exhaust emissions and other airport-related contributions to ambient air pollution: A review. *Atmospheric Environment, 95*, 409–455. https://doi.org/10.1016/j.atmosenv.2014.05.070

MOE (Ministry of the Environment). (2003). Human Health Risk of Mercury. Available (in Japanese) at www.env.go.jp/council/toshin/t07-h1503/mat_02-3.pdf

Morton-Bermea, O., Hernández-Álvarez, E., González-Hernández, G., Romero, F., Lozano, R., & Beramendi-Orosco, L. E. (2015). Assessment of heavy metal pollution in urban topsoils from the metropolitan area of Mexico City. *Journal of Geochemical Exploration, 101*(3), 218–224. https://doi.org/10.1016/j.gexplo.2008.07.002

Morton-Bermea, O., Castro-Larragoitia, J., Arellano-Álvarez, A. A., Pérez-Rodríguez, R. J., Leura-Vicencio, A., Schiavo, B., Salgado-Martínez, E., Razo-Soto, I., & Hernández-Álvarez, E. (2021a). Mercury in blood of children exposed to historical residues from metallurgical activity. *Exposure & Health, 13*(281), 292. https://doi.org/10.1007/s12403-021-00382-z

Morton-Bermea, O., Schiavo, B., Salgado-Martínez, E., Almorín-Ávila, M. J., & Hernández-Álvarez, E. (2021b). Gaseous elemental mercury (GEM) in the Mexico City Metropolitan Area. *Bulletin of Environmental Contamination and Toxicology, 107*, 514–518. https://doi.org/10.1007/s00128-021-03293-6

Osawa, T., Ueno, T., & Fu, F. (2007). Sequential variation of atmospheric mercury in Tokai-mura, seaside area of eastern central Japan. *Journal of Geophysical Research: Atmospheres, 112*. https://doi.org/10.1029/2007JD008538

Ostad-Ali-Askari, K., & Shayannejad, M. (2021). Quantity and quality modelling of groundwater to manage water resources in Isfahan-Borkhar Aquifer. *Environment, Development and Sustainability, 23*, 15943–15959. https://doi.org/10.1007/s10668-021-01323-1

Ostad-Ali-Askari, K., Shayannejad, M., & Ghorbanizadeh-Kharazi, H. (2017). Artificial neural network for modeling nitrate pollution of groundwater in marginal area of Zayandeh-rood River, Isfahan, Iran. *KSCE Journal of Civil Engineering, 21,* 134–140. https://doi.org/10.1007/s12205-016-0572-8

Ostad-Ali-Askar, K., Su, R., & Liu, L. (2018). Water resources and climate change. *Journal of Water and Climate Change, 9*(2), 239. https://doi.org/10.2166/wcc.2018.999

Park, J.-D., & Zheng, W. (2012). Human exposure and health effects of inorganic and elemental mercury. *Journal of Preventive Medicine & Public Health, 45*, 344–352. https://doi.org/10.3961/jpmph.2012.45.6.344

Pirrone, N., Cinnirella, S., Feng, X., Finkelman, R. B., Friedli, H. R., Leaner, J., Mason, R., Mukherjee, A. B., Stracher, G. B., Streets, D. G., & Telmer, K. (2010). Global mercury emissions to the atmosphere from anthropogenic and natural sources. *Atmospheric Chemistry and Physics, 10*, 5951–5964. https://doi.org/10.5194/acp-10-5951-2010

Presto, A. A., & Granite, E. J. (2006). Survey of catalysts for oxidation of mercury in flue gas. *Environmental Science and Technology, 40*(18), 5601–5609. https://doi.org/10.1021/es060504i

Retama, A., Neri-Hernández, A., Jaimes-Palomera, M., Rivera-Hernández, O., Sánchez-Rodríguez, M., López-Medina, A., & Velasco, E. (2019). Fireworks: A major source of inorganic and organic aerosols during Christmas and New Year in Mexico City. *Atmospheric Environmental: X, 2*, 100013. https://doi.org/10.1016/j.aeaoa.2019.100013

Retama, A., Baumgardner, D., Raga, G. B., McMeeking, G. R., & Walker, J. W. (2015). Seasonal and diurnal trends in black carbon properties and co-pollutants in Mexico City. *Atmospheric Chemistry and Physics, 15*, 9693–9709. https://doi.org/10.5194/acp-15-9693-2015

Rutter, A. P., Snyder, D. C., Stone, E. A., Schauer, J. J., Gonzalez-Abraham, R., Molina, L. T., Márquez, C., Cárdenas, B., & de Foy, B. (2009). In situ measurements of speciated atmospheric mercury and the identification of source regions in the Mexico City Metropolitan Area. *Atmospheric Chemistry and Physics, 9*, 207–220. https://doi.org/10.5194/acp-9-207-2009

Schiavo, B., Morton-Bermea, O., Salgado-Martinez, A., & J., Hernández-Álvares, E. (2020a). Estimates of mercury flux and temporal variability of Hg/SO_2 ratio in the plume of Popocatépetl volcano (Mexico). *Journal of South American Earth Sciences, 101*, 102614. https://doi.org/10.1016/j.jsames.2020.102614

Schiavo, B., Morton-Bermea, O., Salgado-Martinez, E., & Hernández-Álvarez, E. (2020b). Evaluation of possible impact on human health of atmospheric mercury emanations from the Popocatépetl volcano. *Environmental Geochemistry and Health, 42*, 3717–3729. https://doi.org/10.1007/s10653-020-00610-6

Schroeder, W. H., & Munthe, J. (1998). Atmospheric mercury – An overview. *Atmospheric Environment, 32*, 809–822. https://doi.org/10.1016/S1352-2310(97)00293-8

Seo, Y.-S., Jeong, S.-P., Holsen, T. M., Han, Y.-J., Choi, E., Park, E. H., Kim, T. Y., Eum, H.-S., Park, D. G., Kim, E., Kim, S., Kim, J.-H., Choi, J., & Yi, S.-M. (2016). Characteristics of total gaseous mercury (TGM) concentrations in an industrial complex in South Korea: Impacts from local sources. *Atmospheric Chemistry and Physics, 16*, 10215–10228. https://doi.org/10.5194/acp-16-10215-2016

Sholupov, S. E., & Ganeyev, A. A. (1995). Zeeman absorption spectrometry using high frequency modulated light polarization. *Spectrochimica Acta Part b: Atomic Spectroscopy, 50*, 1227–1238. https://doi.org/10.1016/0584-8547(95)01316-7

Si, L., & Ariya, P. A. (2018). Recent advances in atmospheric chemistry of mercury. *Atmosphere, 9*(2), 76. https://doi.org/10.3390/atmos9020076

Spreadbury, C. J., Clavier, K. A., Lin, A. M., & Townsend, T. G. (2021). A critical analysis of leaching and environmental risk assessment for reclaimed asphalt pavement management. *Science of the Total Environment, 775*, 145741. https://doi.org/10.1016/j.scitotenv.2021.145741

Sizmur, T., McArthur, G., Risk, D., Tordon, R., & O'Driscoll, N. J. (2017). Gaseous mercury flux from salt marshes is mediated be solar radiation and temperature. *Atmospheric Environment, 153*, 117–125. https://doi.org/10.1016/j.atmosenv.2017.01.024

Sosa, G., Vega, E., González-avalos, E., Mora, V., & López-Veneroni, D. (2013). Air pollutant characterization in Tula Industrial Corridor, Central Mexico, during the MILAGRO study. *BioMed Research International, 2013*(521728), *13*. https://doi.org/10.1155/2013/521728

Sprovieri, F., Pirrone, N., Ebinghaus, R., Kock, H., & Dommergue, A. (2010). A review of worldwide atmospheric mercury measurements. *Atmospheric Chemistry and Physics, 10*, 8245–8265. https://doi.org/10.5194/acp-10-8245-2010

Sprovieri, F., Pirrone, N., Bencardino, M., D'Amore, F., Carbone, F., Cinnirella, S., Mannarino, V., Landis, M., Ebinghaus, R., Weigelt, A., Brunke, E.-G., Labuschagne, C., Martin, L., Munthe, J., Wängberg, I., Artaxo, P., Morais, F., Barbosa, H. D. M. J., Brito, J., … Norstrom, C. (2016). Atmospheric mercury concentrations observed at ground-based monitoring sites globally distributed in the framework of the GMOS network. *Atmospheric Chemistry and Physics, 16*, 11915–11935. https://doi.org/10.5194/acp-16-11915-2016

Stein, A. F., Draxler, R. R., Rolph, G. D., Stunder, B. J. B., Cohen, M. D., & Ngan, F. (2015). NOAAs HYSPLIT atmospheric transport and dispersion modeling system. *Bulletin of the American Meteorological Society, 96*, 205977. https://doi.org/10.1175/BAMS-D-14-00110.1

Swartzendruber, P. C., Jaffe, D. A., Prestbo, E. M., Weiss-Penzias, P., Selin, N. E., Park, R., Jacob, D. J., Strode, S., & Jaeglé, L. (2006). Observations of reactive gaseous mercury in the free troposphere at the Mount Bachelor Observatory. *Journal of Geophysical Research: Atmospheres, 111*. https://doi.org/10.1029/2006JD007415

Talebmorad, H., Abedi-Koupai, A., Eslamian, S., Mousavi, S.-F., Akhavan, S., Ostad-Ali-Askari, O., & Singh, V. P. (2021). Evaluation of the impact of climate change on reference crop evapotranspiration in Hamedan-Bahar Plain. *International Journal of Hydrology Science and Technology, 11*(3), 333–347. https://doi.org/10.1504/IJHST.2021.114554

UNEP. (2013). Minamata Convention on Mercury – Text and Annexes, UNEP, Geneva, Switzerland, 1–59.

U.S. Department of Health and Human Services, Public Health Service, ATSDR. (2012). *Toxicological Profile for Mercury* (pp. 1–600). U.S. Department of Health and Human Services, Atlanta, GA, USA. https://www.atsdr.cdc.gov/mercury/docs/11-229617-E-508_HealthEffects.pdf

USDOE. (2011). The risk assessment information system (RAIS). Cass Avenue Argonne, IL: U.S. Department of Energy's Oak Ridge Operations Office (ORO).

USEPA. (1989). Risk Assessment Guidance for Superfund, Vol. I, Human Health Evaluation Manual (Part A), EPA/540/1–89/002. Office of Emergency and Remedial Response, Washington, DC.

USEPA. (2001). Methods for collection, storage and manipulation of sediments for chemical and toxicological analyses. Technical Manual, EPA-823-B-01–002, Office of Water, Washington, DC.

USEPA. (2002). *Supplemental guidance for developing soil screening levels for superfund sites*. U.S. Environmental Protection Agency, Office of Emergency and Remedial Response.

USEPA. (2009). Risk Assessment Guidance for Superfund Volume I: Human Health Evaluation Manual (Part F, Supplemental Guidance for Inhalation Risk Assessment (EPA-540-R-070-002). Office of Superfund Remediation and Technology Innovation, Washington D.C. https://www.epa.gov/sites/production/files/2015-09/documents/partf_200901_final.pdf

USEPA. (2011). *Integrated risk information system (IRIS)*. Environmental Protection Agency.

USEPA. (2020). Regional Screening Levels (RSLs) - Resident Ambient Air Table (TR¼1E-06, HQ¼1). Center for Public Health and Environmental Assessment, Washington, DC. https://semspub.epa.gov/work/HQ/199934.pdf

Vaselli, O., Higueras, P., Nisi, B., Esbrí, J. M., Cabassi, J., Martínez-Coronado, A., Tassi, F., & Rappuoli, D. (2013). Distribution of gaseous Hg in the mercury mining district of Mt. Amiata (Central Italy): A geochemical survey prior the reclamation project. *Environmental Research, 125*, 179–187. https://doi.org/10.1016/j.envres.2012.12.010

Velasco, A., Arcega-Cabrera, F., Oceguera-Vargas, I., Ramírez, M., Ortinez, A., Umlauf, G., & Sena, F. (2016). Global Mercury Observatory System (GMOS): Measurements of atmospheric mercury in Celestun, Yucatan, Mexico during 2012. *Environmental Science and Pollution Research, 23*, 17474–17483. https://doi.org/10.1007/s11356-016-6852-5

Wang, C., Wang, Z., & Zhang, X. (2021). Speciated atmospheric mercury during haze and non-haze periods in winter at an urban site in Beijing, China: Pollution characteristics, sources, and causes analyses. *Atmospheric Research, 247*, 105209. https://doi.org/10.1016/j.atmosres.2020.105209

Wang, F., Wang, S., Zhang, L., Yang, H., & Wu, Q. (2016). Characteristics of mercury cycling in the cement production process. *Journal of Hazardous Materials, 302*, 27–35. https://doi.org/10.1016/j.jhazmat.2015.09.042

Weiss-Penzias, P., Jaffe, D.A., Swartzendruber, P., Dennison, J.B., Chand, D., Hafner, W., & Prestbo, E. (2006). Observations of Asian air pollution in the free troposphere at Mount Bachelor Observatory during the spring of 2004. *Journal of Geophysical Research: Atmosphere, 111*. https://doi.org/10.1029/2005JD006522

WHO. (2000). Air Quality Guideline for Europe. 2nd ed.. World Health Organization. Regional Office for Europe. https://apps.who.int/iris/handle/10665/107335

WHO. (2003). Environmental mercury and inorganic mercury compounds: Human health aspects. https://apps.who.int/iris/bitstream/handle/10665/42607/9241530502.pdf

Wdowin, M., Wiatros-Motyka, M. M., Panek, R., Stevens, L. A., Franus, W., Snape, C. E (2014). Experimental study of mercury removal from exhaust gases. *Fuel*, *128*, 415–457. https://doi.org/10.1016/j.fuel.2014.03.041

Won, J. H., Park, J. Y., & Lee, T. G. (2007). Mercury emissions from automobiles using gasoline, diesel, and LPG. *Atmospheric Environment, 41*, 7547–7552. https://doi.org/10.1016/j.atmosenv.2007.05.043

Yang, H., Xu, Z., Fan, M., Bland, A. E., & Judkins, R. R. (2007). Adsorbents for capturing mercury in coal-fired boiler flue gas. *Journal of Hazardous Materials, 146*(2), 1–11. https://doi.org/10.1016/j.jhazmat.2007.04.113

Ye, Z., Mao, H., Lin, C.-J., & Kim, S. Y. (2016). Investigation of processes controlling summertime gaseous elemental mercury oxidation at midlatitudinal marine, coastal, and inland sites. *Atmospheric Chemistry and Physics, 16*, 8461–8478. https://doi.org/10.5194/acp-16-8461-2016

Yuan, C.-S., Jhang, Y.-M., Ie, I.-R., Lee, C.-E., Fang, G.-C., & Luo, J. (2021). Exploratory investigation in spatiotemporal

variation and source identification of atmospheric speciated mercury surrounding the Taiwan Strait. *Atmospheric Pollution Research, 12*, 54–64. https://doi.org/10.1016/j.apr.2021.01.015

Yue, F., Qui, Y., Zhan, H., Kang, H., Li, J., Liu, C., & Xie, Z. (2021). Characteristics of gaseous elemental mercury and its corresponding source contributions to regional transport in Hefei, China. *Atmospheric Pollution Research, 12*, 101146. https://doi.org/10.1016/j.apr.2021.101146

Zhang, H., Fu, X., Lin, C.-J., Shang, L., Zhang, Y., Feng, X., & Lin, C. (2016). Monsoon-facilitated characteristics and transport of atmospheric mercury at a high-altitude background site in southwestern China. *Atmospheric Chemistry and Physics, 16*, 13131–13148. https://doi.org/10.5194/acp-16-13131-2016

Zhang, L., Wang, S., Wang, L., Wu, Y., Duan, L., Wu, Q., Wang, F., Yang, M., Yang, H., Hao, J., & Liu, X. (2015). Updated emission inventories for speciated atmospheric mercury from anthropogenic sources in China. *Environmental Science and Technology, 49*(5), 3185–3194. https://doi.org/10.1021/es504840m

Zhou, J., Wang, Z., Zhang, X., Driscoll, C. T., & Lin, C.-J. (2020). Soil–atmosphere exchange flux of total gaseous mercury (TGM) at subtropical and temperate forest catchments. *Atmospheric Chemistry and Physics, 20*, 16117–16133. https://doi.org/10.5194/acp-20-16117-2020